Available online at www.sciencedirect.com
SCIENCE DIRECT®
Talanta 62 (2004) 299–305
Talanta
www.elsevier.com/locate/talanta

Three-way chemometric method study and UV-Vis absorbance for the study of simultaneous degradation of anthocyanins in flowers of the *Hibiscus rosa-sinensys* species

Maria Alice B. Levi [a], Ieda S. Scarminio [a,*], Ronei J. Poppi [b], Marcello G. Trevisan [b]

[a] *Departamento de Química, Universidade Estadual de Londrina, C.P. 6001, CEP 86051-970, Londrina, PR, Brazil*
[b] *Instituto de Química, Universidade Estadual de Campinas, C.P. 6154, CEP 13083-970, Campinas, SP, Brazil*

Received 16 April 2003; received in revised form 11 July 2003; accepted 24 July 2003

Abstract

Ultraviolet-visible spectra of flower extracts of the *Hibiscus rosa-sinensys* L. var. regius maximus species have been measured between 240.02 and 747.97 nm at pH values ranging from 1.1 to 13.0. Deconvolution of these spectra using the Parallel Factor Analysis (PARAFAC) model permitted the study of anthocyanin systems without isolation and purification of the individual species. Seven species were identified: flavilium cation, carbinol, quinoidal base, and E and Z-chacone and their ionized forms. The concentration changes of flavilium cation, quinoidal basen, and E and Z ionized chalcones were determined as function of pH at the different wavelengths. The flavilium cation, quinoidal base, and ionized E-clacone are involved in tho stage kinetic processes, a fast one followed by a slower one. Ionized Z-chalcone obeys a simple first-order processes. The spectral profiles recovered by PARAFAC model are in excellent agreement with bands of experimental spectra reported in the literature for the individual species measured at specific pH values. These results complement those obtained using chemical and simple mathematical techniques and demonstrate how chemometric methods can resolve problems for complex systems.

Keywords: Kinetic-spectrophotometric; PARAFAC; Anthocyanins

1. Introduction

Anthocyanins are natural pigments, responsible for the brilliant orange, pink, scarlet, red, mauve, magenta, violet, and blue colors of flowers petals, vegetables, and fruits. They are structurally characterized by possessing a $C_6C_3C_6$ carbon skeleton, Fig. 1 [1].

There is widespread interest in anthocyanin applications and their degradation reactions in many fields of science. For example: the most important industrial application of plant anthocyanin research is in the food industry, and especially for wine commercialization [2]. They have been postulated as chemical markers capable of differentiating grape cultivars and reed wines made with different grape cultivars [3]. Another major interest of the food industry is in their use as natural colorants to replace synthetic red dyes [2]. Recently, the biological activities of anthocyanin, such as its antioxidant activity, protection ability from atherosclerosis, and anti-carcinogenic activity have been investigated, and shown to have some beneficial effects in the treatment of diseases [4]. These pigment patterns exhibited by different fruit species can be interesting for chemotaxonomic investigations and are now useful for controlling juice mixture or juice adulteration [5].

One of the most important functions of anthocyanins in the area of visible perception is its attraction of animals, mainly insects and birds for the purpose of pollination and seed dispersal. Therefore, they are extremely valuable in plant–animal interactions [6].

It has long been known that anthocyanins bearing the same chromophoric structure can give rise to different colors, depending on several chemical and physical factors, such as temperature, pH, solvent, and the presence of other molecules which can generally be described as copigments [6,7]. The main factor in the fadin process is the high reactivity of the flavylium cation toward nucleophilic reagents,

* Corresponding author. Tel.: +55-43-371-4366; fax: +55-43-328-4440.
E-mail address: ieda@iqm.uel.br (I.S. Scarminio).

0039-9140/$ – see front matter © 2003 Elsevier B.V. All rights reserved.
doi:10.1016/j.talanta.2003.07.015

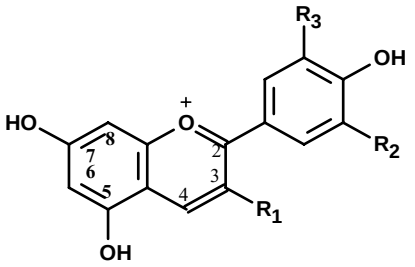

Fig. 1. Chemical structure of anthocyanins. R_1 is glycosil. R_2 and R_3 are usually H, OH, or OCH_3.

including the three water species (H_2O, OH^-, and H^+) [8]. Thus, water solvent plays an important role in influencing both the stability and reactivity of the anthocyanins. This demonstrates that pH is one of the most important factors in the phenomenon of flower and fruit pigmentation due to anthocyanins [9]. The chemical structure of the pigments is also one of the factors which affects the anthocyanins colors. Depending on the degree of acidity or alkalinity, anthocyanins adopt different chemical structures, including the flavylium cation (AH^+), the quinoidal bases (A), the pseudobase or carbinol (B), and the chalcones (C) (Fig. 2).

The difficulty with studying anthocyanin degradation reactions is to find robust techniques for the identification of structurally similar compounds and elucidate the mechanism of degradation without separation of the plant components. Until now, traditional studies on degradation reactions as well as on the copigmentation effect of flowers and fruits, involve compound extraction, isolation and purification [10]. They are generally isolated as flavylium cations, the counter-ion being the chloride or perclorate anion.

Modern analytical instrumentation and chemometric methods are capable of studying anthocyanin systems without isolation and purification of individual components.

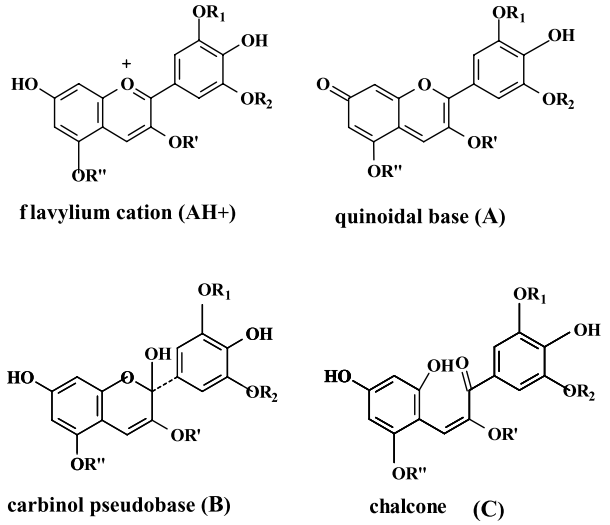

Fig. 2. Molecular structures of the flavylium cation (AH^+), quinoidal base (A), pseudobase or carbinol (B), and chalcone (C). R′ is glycosil and R″ are usually and H or sugar. R_1 and R_2 are usually H, OH, or OCH_3.

In the last two decades multi-dimentional data arrays can be obtained using so-called hyphenated instruments such as a high-performance liquid chromatography with a diode array detector (HPLC-DAD), an excitation/emission matrix spectrofluorometer, or a UV-Vis spectrophotometer equipped with a diode array detector for the in-acquisition of spectra as function of reaction time. In this way each sample generates a two-way data matrix (spectra versus time). Thus far, several multi-way methods have been developed to solve complex chemical problems, such as Partial Least Squares (PLS three way) [11,12], Generalized Rank Annihilation Method (GRAM) [13], Direct Trilinear Decomposition (TLD) [14], Tucker [15], Parallel Factor Analysis (PARAFAC) [16].

In the acidic medium the experimental results have usually been interpreted in terms of the following isolated structures: flavylium cation, carbinol, and chalcone. The colour intensities are measured as absorbance values at $\lambda_{vis\text{-}max}$ for each individual pigment at its appropriate pH value. In contrast the objective of this work is to measure complete UV-Vis spectra between 240.02 and 747.97 nm for values between 1.1 and 13.0. Deconvolution of these spectra using the PARAFAC model permits the study of anthocyanin systems without isolation and purification of the individual components.

The PARAFAC model was applied to resolve the absorption spectral profiles as well as the kinetic concentration profiles, resulting in relative concentration profiles as a function of pH, giving a real-world example of the resolution of a complex multi-component kinetic system. The pigment mixtures including anthocyanins and other substances, namely, flavone, glycosides (copigments), and free sugars, were extracted from fresh petals of hibiscus flowers of the *Hibiscus rosa-sinensys* L. var. regius maximus species. The results obtained in this work may constitute the basis for the development of an analytical methodology for determining the number of species involved and their degradation kinetics.

2. Theory

Parallel Factor Analysis (PARAFAC) [16] is a decomposition method for multi-way data which performs deconvolution in three loadings matrices, $\boldsymbol{A}$, $\boldsymbol{B}$, and $\boldsymbol{C}$ with elements a_{if}, b_{jf}, and c_{kf} Eq. (1). The trilinear model is found to minimize the sum of squares of the residuals, e_{ijk}, in the model,

$$x_{ijk} = \sum_{f=1}^{F} a_{if} b_{jf} c_{kf} + e_{ijk} \quad (1)$$

where x_{ijk} is the (i, j, k) original element of the trilinear data set, and F is the number of factors.

The interactive algorithm used to solve the PARAFAC model is alternating least squares (ALS) that assumes the loadings in two modes and then estimates the unknown set of parameters of the last mode until optimizing the residuals of the model. When the model converges, the results have

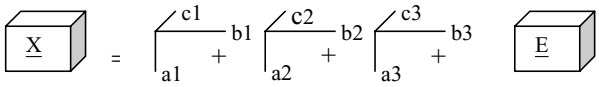

Fig. 3. Decomposition of the three-way data array for PARAFAC using three components.

the same number of triads as the number of factors assumed. Each triad is composed of three orthogonal vectors that have the profile of the pure species present in the system.

A graphic representation of decomposition with PARAFAC is shown in Fig. 3. In this figure, the vectors $\boldsymbol{a_1}$, $\boldsymbol{a_2}$, and $\boldsymbol{a_3}$ form the $\boldsymbol{A}$ loading matrix, the vectors $\boldsymbol{b_1}$, $\boldsymbol{b_2}$, and $\boldsymbol{b_3}$ form the $\boldsymbol{B}$ loading matrix, and the vectors $\boldsymbol{c_1}$, $\boldsymbol{c_2}$, and $\boldsymbol{c_3}$ form the $\boldsymbol{C}$ loading matrix.

The critical problem for determining the PARAFAC model is the correct choice of the number of factors for decomposition. This is done with experimental analyst knowledge and using techniques such as split-half experiments [17] and estimation of core consistency that have been shown to be efficient.

In the split-half experiments, a type of jack-knife validation, the data set is split into several sub-blocks and then PARAFAC is performed on each sub-block. Owing to the uniqueness of the PARAFAC model the identical loadings on sub-blocks will be obtained if the correct number of factors (analytes) was chosen.

3. Experimental

3.1. Plant material

Plants were cultivated in the garden of the Chemistry Department of the Universidade Estadual de Londrina (UEL), in Londrina, PR, Brazil.

Voucher was deposited in the herbarium of the Universidade Estadual de Londrina. The access numbers is FUEL 33818.3.2.

3.2. Extract preparation

Pigments were extracted by maceration of fresh petals (11.80 g) of the hibiscus flowers with 0.1% HCl in ethyl alcohol. The ethanolic extracts were filtered with filter paper.

3.3. Buffer solutions

All regents were of analytical grade. Buffer solutions with 14 different pH values were prepared in accordance with Table 1. The pH of each solution was measured with a HANNA HI model HI9321 pH Meter.

3.4. Spectrophotometric analysis

The analyses were carried out using an Ocean Optics model CHEM2000 Spectrophotometer with a quartz cuvette ($d = 1$ cm). The temperature was fixed at 25 (± 0.1) °C. Ultraviolet-visible absorption spectra at different pH values, were recorded from 240.02 to 747.97 nm, with increments of 0.38 nm. Three milliliter of ethanolic extracts of anthocyanin were added to 20 ml buffer solutions, and immediately recorded at intervals of 1 s over 30 min.

3.5. Data analysis

Each spectrum was reduced from 1450 to 261 points to lower the dimension of the three-way data matrices and each experiment was composed of 121 spectra. A set of 14 pH values was used to construct the model. The kinetic data collected was arranged in a three-way array with dimensions of $14 \times 261 \times 121$ (pH, wavelength, and time, respectively).

3.6. Computer programs

The experimental data were processed with programs written in Matlab 5.0. The PARAFAC program was developed by Ramus Bro and Claus Andersson and is available at http/www.models.kvl.dk/source/.

Table 1
Solvent proportions (v/v) used to prepare the 14 different buffer solutions in the 1.1–13.0 pH region

pH	HCl (0.10 mol l^{-1})	KH_2PO_4 (0.15 mol l−1)	Na_2HPO_4 (0.15 mol l−1)	K_3PO_4 (0.15 mol l−1)	NaOH (10%)
1.1	9.5	0.5	–	–	–
3.2	0.5	9.5	–	–	–
4.6	–	10.0	–	–	–
5.2	–	9.5	0.5	–	–
5.8	–	9.0	1.0	–	–
6.1	–	8.0	2.0	–	–
6.5	–	6.0	4.0	–	–
6.9	–	4.0	6.0	–	–
7.1	–	3.0	7.0	–	–
7.5	–	1.0	9.0	–	–
7.9	–	5.0	–	5.0	–
10.3	–	4.0	–	6.0	–
11.4	–		3.0	7.0	–
13.0	–		–	–	10.0

4. Results and discussion

Fig. 4 shows the experimental surfaces obtained at different pH values. In acidic medium, at pH 1.0 (Fig. 4a) and pH 3.2 (Fig. 4b) the spectra shows a characteristic absorption of the cation form of the flavilium structure, with a strong peak absorption band at $\lambda_{max} = 514$ nm. Chalcone absorbs strongly in the 300–400 nm region and less strongly in the 220–270 nm region. Close to 275 nm the peak absorption is characteristic of the carbinol base B structure. 5-Glycosides and 3,5-diglycosides, on the other hand, show merely an inflection of low intensity at 440 nm. At decreased acidity, in weakly acidic, and neutral buffer solutions, pH 4.7 and 7.0, the spectra ceases to show a flavylium structure absorption band, Fig. 4c and 4d. As can be seen from the spectrum at pH 4.7, light absorption leads to colour bleaching and degradation of the anthocyanin molecules, as evidenced by decreases of absorption with maxima at 514 and 278 nm assigned to

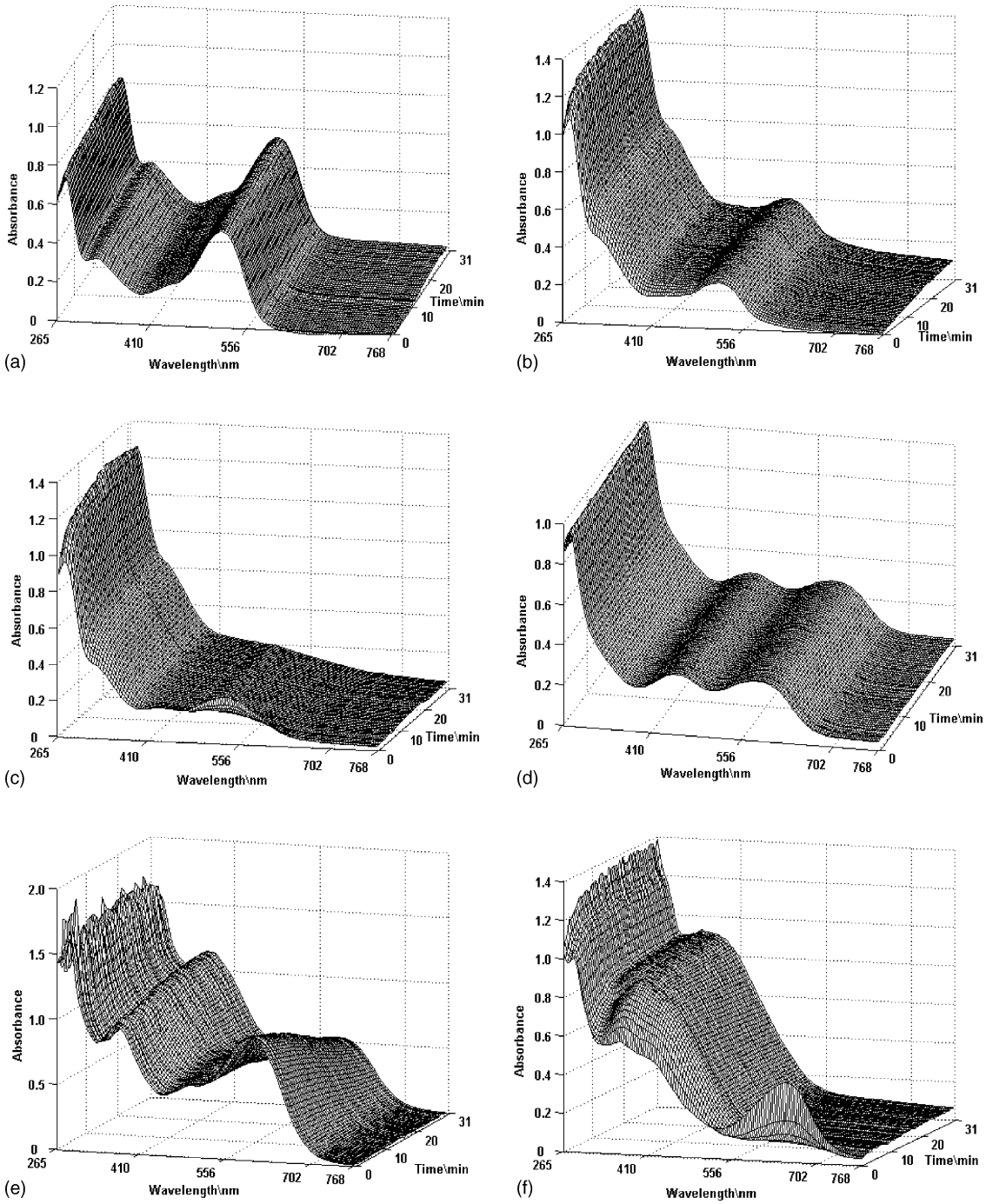

Fig. 4. Three-way spectral data matrices corresponding to the following pH values: (a) pH 1.0; (b) pH 3.2; (c) pH 4.7; (d) pH 7.1, (e) pH 11.4, and (f) pH 13.0.

the flavylium cation and carbinol pseudobase, respectively. At pH 7.0 two news bands appear at around 550 and 440 nm. These maxima indicate anhydrobase and ionized chalcone, respectively. On other hand, the observed spectra at pH 11.4 and 13.0 show three bands, that correspond to an ionized anhydrobase, A^-, ($\lambda_{max} = 600$ nm), ionized Z-chalcone, C_Z^-, ($\lambda_{max} = 350$ nm) and E^--chalcone, C_E^-, ($\lambda_{max} = 430$ nm).

The number of components used in the construction of the model was based on percentage of fit calculations. This percentage value corresponds to how well the model can reproduce the experimental data and is given by

$$\text{Fit percent} = 100 \times \left(1 - \frac{\sum_{i=1}^{I}\sum_{j=1}^{J}\sum_{k=1}^{K}(x_{ijk} - \hat{x}_{ijk})^2}{\sum_{i=1}^{I}\sum_{j=1}^{J}\sum_{k=1}^{K}x_{ijk}^2}\right) \quad (2)$$

where x_{ijk} is the ijk-th experimental element and $\hat{x}_{ijk}$ the ijk-th element predicted by the model.

In this case, four was considered to be an adequate number of components for construction of the PARAFAC model, because the percentage fit was 99%.

The PARAFAC model obtained with four components decomposes the tensor X into a loading matrix of spectral profiles ($\boldsymbol{A}$), loading matrices of kinetic profiles ($\boldsymbol{B}$) and loading matrix of relative concentrations ($\boldsymbol{C}$). Fig. 5 shows a graph of the loadings corresponding to the first dimension of the three-way tensor X. This $\boldsymbol{A}$ matrix is formed by four loadings vectors, $\boldsymbol{a_1}$, $\boldsymbol{a_2}$, $\boldsymbol{a_3}$, and $\boldsymbol{a_4}$. Each one furnishes the resolved spectral profiles at the PARAFAC model applied to the full array. By comparing these spectra it is possible to confirm the structural changes occurring in the 1.1–13.0 pH range. Seven chemical species are easily recognized in the spectra in Fig. 5. The absorption spectrum of the *trans*-chalcone and *cis*-chalcone isomers, are practically identical. In spite of this the PARAFAC model was able to separate the absorption bands of these isomers in their ionized forms. These spectra show no evidence of the presence of ionized anhydrobase. In fact this species forms as an intermediate. In this study, good agreement between the resolved spectra profiles and reported spectra profiles [18] is obtained.

Fig. 6 shows a graph of the loadings corresponding to the second dimension of the three-way X tensor. This $\boldsymbol{B}$ matrix shows that, in the 1.1–13.0 pH range, there are four kinetically distinct processes, formed by four loadings vectors, $\boldsymbol{b_1}$, $\boldsymbol{b_2}$, $\boldsymbol{b_3}$, and $\boldsymbol{b_4}$. Each one furnishes the kinetic profile of the corresponding loading vector shown in Fig. 5.

From a kinetic viewpoint, the situation encountered in this process is interesting since the reported investigations are limited to an acidic pH range in which no ionized chalcone form and quinoidal base A and Z-chalcones are present.

For the first loading vector, $\boldsymbol{b_1}$, the kinetic behavior is described by the equation

$$y = y_0 + A_1(1 - e^{-t/k_1}) + A_2(1 - e^{-t/k_2}) \quad (3)$$

where y_0, A_1, A_2, k_1, and k_2 are $6.60 \times 10^{-2} \pm 2.10 \times 10^{-4}$, $8.60 \times 10^{-3} \pm 8.40 \times 10^{-4}$, $2.55 \times 10^{-2} \pm 7.70 \times 10^{-4}$, 106.88 ± 11.80, and 528.57 ± 21.47, respectively. Value of chi-square χ^2 was 1.14×10^{-7}. These parameters and their errors were obtained by performing a non-linear curve fit of the loadings as a function of times, in seconds, using the ORIGIN computer program. In this equation, two process behaviors are observed. Both processes obey first-order kinetics and they have quite different rates. The first process is fast with increasing absorbance, followed by a slower

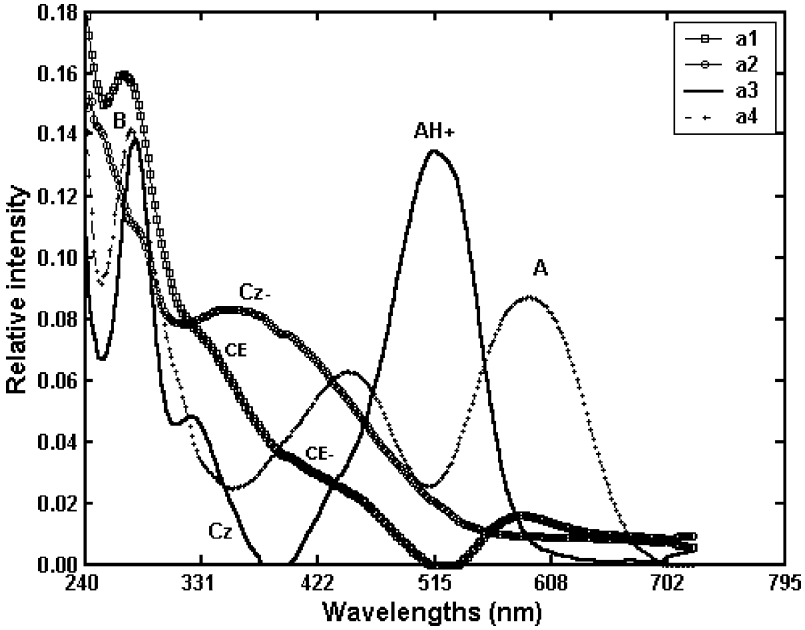

Fig. 5. Spectral profiles recovered by the PARAFAC model at different pH values based on the deconvolution of UV-Vis absorption spectra, featuring the various anthocyanin secondary monomeric forms.

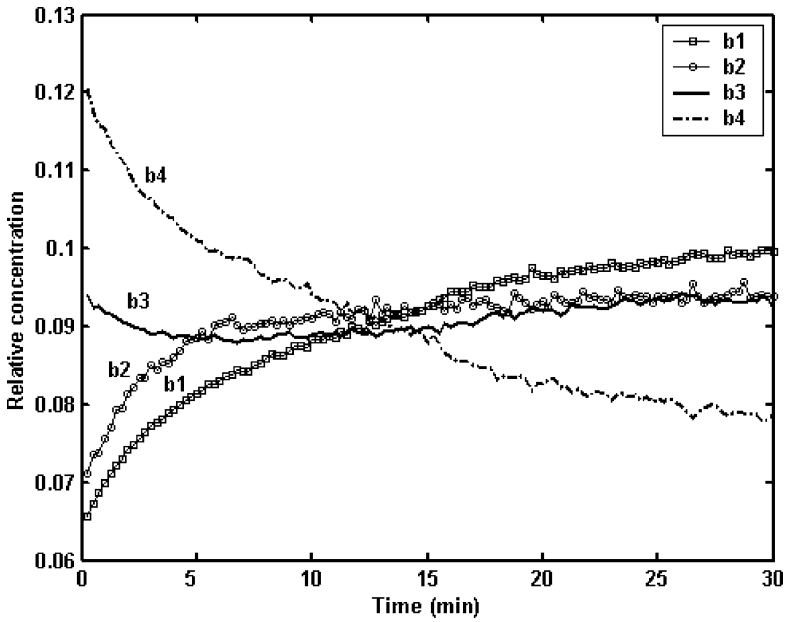

Fig. 6. Kinetic profiles obtained by the PARAFAC model at different pH values based on the deconvolution of UV-Vis absorption spectra.

process for which it decreases. This behavior can be observed for the correspondent loadings vector, $\boldsymbol{c_1}$ in Fig. 7. Although the above values can not be compared directly with results in the literature, McClelland and Gedge [19] have reported a two phase behavior for flavylium perchlorates.

For the second loading vector $\boldsymbol{b_2}$, Fig. 6 the kinetic behavior is described by equation

$$y = A_1 - A_2\,e^{-k_2 t} \tag{4}$$

where A_1, A_2, and k are $9.33 \times 10^{-2} \pm 1.00 \times 10^{-4}$, $2.12 \times 10^{-3} \pm 4.10 \times 10^{-4}$, $6.81 \times 10^{-3} \pm 2.20 \times 10^{-4}$, respectively. Value of χ^2 was 6.63×10^{-7}. This behavior obeys first-order kinetics. The associated concentration loading vector, $\boldsymbol{c_2}$, is shown in Fig. 7. The absorption increases in the spectral region, corresponding to the loading vector, $\boldsymbol{a_2}$, in Fig. 5 is characteristic by ionized Z-chalcone.

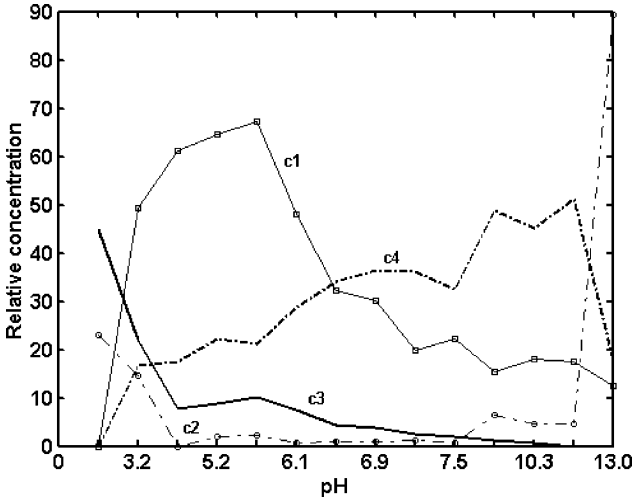

Fig. 7. Concentration profiles obtained by the PARAFAC model at different pH values based on the deconvolution of UV-Vis absorption spectra.

For the third $\boldsymbol{b_3}$ loading vector, two process kinetic behaviors are observed. The absorption spectra $\boldsymbol{a_3}$ loading vector, Fig. 5, is characteristic of the flavylium cation. Its disappearance, however, does not obey only first-order kinetics. Two almost separate kinetic processes occur. The first fast phase has absorbance decreases in the first 4 min described by the equation

$$y = y_0 + A_1\,e^{-kt} \tag{5}$$

where y_0, A_1, A_2, and k are $8.81 \times 10^{-2} \pm 2.0 \times 10^{-4}$, $5.56 \times 10^{-3} \pm 2.10 \times 10^{-4}$, and $7.27 \times 10^{-1} \pm 8.7 \times 10^{-2}$, respectively. Value of χ^2 was 7.70×10^{-8}. The second is a slower phase in which it increases linearly with a $2.47 \times 10^{-4} \pm 6.50 \times 10^{-6}$ slope indicating that the kinetics does not depend on the concentration of the flavylium cation any more. The associated concentration loading vector, $\boldsymbol{c_4}$, is shown in Fig. 7.

For the fourth loading vector, $\boldsymbol{b_4}$, the kinetic behavior is described by equation

$$y = y_0 + A_1\,e^{-t/k_1} + A_2\,e^{-t/k_2} \tag{6}$$

where y_0, A_1, A_2, k_1, and k_2 are $7.74 \times 10^{-2} \pm 2.43 \times 10^{-4}$, $9.18 \times 10^{-3} \pm 2.50 \times 10^{-7}$, $3.32 \times 10^{-2} \pm 5.70 \times 10^{-5}$, 74.69 ± 9.63, and 572.67 ± 20.30, respectively. Value of χ^2 was 8.70×10^{-6}. In this equation, two process behaviors are observed. Both phases obey first-order kinetics and are quite different in rate. The absorption spectra loading vector, $\boldsymbol{a_4}$, Fig. 5, is characteristic of quinoidal base. The associated concentration loading vector $\boldsymbol{c_4}$ is shown in Fig. 7.

5. Conclusions

In this study, the kinetics of simultaneous degradation of anthocyanins in extract from fresh petals of hibiscus flowers of the *Hibiscus rosa-sinensys* L. var. regius maximus species was studied using a PARAFAC analysis of three-way data, without the physical–chemical separation of plant components. It has been shown that simple kinetic-spectrophotometric experimental procedures are able to generate trilinear structures from complex reaction structures at different pH values based on the deconvolution of UV-Vis absorption spectra. The spectral profiles recovered by the model are excellent agreement with the experimental spectra confirming the fact that a complex system difficult to analyze using general chemistry and simple mathematical methods can be resolved using chemometric methods.

References

[1] R.L. Jackman, R.Y. Yada, M.A. Tung, R.A. Speers, J. Food Biochem. 11 (1987) 201.
[2] J.B. Harborne, The Flavonoids: Advances in Research Since 1980, Chapman & Hall, New York, 1988, p. 202.
[3] J. Bakker, C.F. Timberlake, J. Sci. Food Agric. 36 (1985) 1315.
[4] Pi.-Jen. Tsai, J. McIntosh, P. Pearce, B. Camden, B.R. Jordan, Food Res. Int. 35 (2002) 351.
[5] J.-P. Goiffon, P.P. Mouly, E.M. Gaydou, Anal. Chim. Acta 382 (1999) 39.
[6] F.O. Obi, I.A. Usenu, J.O. Osayande, Toxicology 13 (1998) 93.
[7] P. Figueiredo, M. Elhabiri, K. Toki, N. Saito, O. Dangles, R. Brouillard, Phytochemistry 41 (1996) 301.
[8] C.E. Lewis, J.R.L. Walker, J.E. Lancaster, Food Chem. 54 (1995) 315.
[9] P. Markakis, Anthocyanins as Food Colors, Academic Press, New York, 1982, p. 17.
[10] R. Brouillard, Phytochemistry 22 (1983) 1311.
[11] L. Stahle, Chemom. Intell. Lab. Syst. 7 (1989) 95.
[12] R. Bro, J. Chemom. 10 (1996) 47.
[13] E. Sanches, R. Kowalski, J. Chemom. 2 (1998) 265.
[14] E. Sanches, R. Kowalski, J. Chemom. 4 (1990) 29.
[15] L.R. Tucker, Psycometrika 31 (1996) 279.
[16] R. Bro, J. Chemom. 38 (1997) 149.
[17] R. Bro, Multiway Analysis in the Food Industry: Models, Algorithms and Applications, Doctoral Dissertation, University of Amsterdam, 1998.
[18] J.B. Harborne, The Flavonoids: Advances in Research Since 1986, Chapman & Hall, New York, 1996, p. 573.
[19] R.A. McClelland, S. Gedge, J. Am. Chem. Soc. 102 (1980) 5838.